

# New and Unusual Bonding in Open Shell van der Waals Molecules Revealed by the Heavy Atom Effect: The Case of BAr

Karl Sohlberg\*<sup>‡</sup> and David R. Yarkony\*<sup>‡</sup>

Department of Chemistry, The Johns Hopkins University, Baltimore, Maryland 21218

Received: November 18, 1996; In Final Form: February 22, 1997<sup>⊗</sup>

Calculations are reported for the excited  $1^4\Pi$  and  $C^2\Delta$  electronic states of BAr and the (nominally  $2s2p^2$ )  $4P$  and  $2D$  states of atomic boron. It was found necessary to extend an augmented valence triple-zeta orbital basis set to correctly describe the  $C^2\Delta$  state. This enhancement is necessitated by the near degeneracy of the valence  $2s2p^2$   $2D$  and Rydberg  $2s^23d$   $2D$  electron configurations in atomic boron, both of which are required to describe BAr  $C^2\Delta$ . Unexpectedly strong bonding in the  $C^2\Delta$  state is found. This bonding is shown to have its root in a type of coordinate covalency, dative bonding, that is sensitive to electron correlation effects and is reflected in a large external heavy atom effect in the spin-orbit coupling of the  $1^4\Pi$  and  $C^2\Delta$  states.

## I. Introduction

Van der Waals complexes are important in many areas of physical chemistry, being for example, relevant to the structure of potential cryogenic propellants,<sup>1</sup> and providing a valuable means for studying chemical reactions with orientational control.<sup>2</sup> A particularly interesting class of these molecules is the open shell van der Waals complex, in which one of the moieties is an open shell species. These molecules, which have received considerable attention recently,<sup>3,4</sup> exhibit a wide range of binding energies.<sup>4</sup>

Recently, as part of an effort to understand the nature of boron doped in cryogenic hydrogen matrices, Dagdigian and co-workers have systematically studied the interactions of the open shell van der Waals molecules formed by boron in its electronic ground state or an excited state with a rare gas or molecular hydrogen.<sup>3,5–8</sup> That research suggested that the  $C^2\Delta$  state of BAr is quite strongly bound but is rapidly predissociated by spin-orbit induced coupling to the repulsive  $1^4\Pi$  state.<sup>8</sup> The later observation may seem counterintuitive since spectroscopic studies suggest the open shell moiety to be a largely unperturbed boron atom which has at best modest spin-orbit interactions. In this work we consider the electronic structure of the electronically excited  $C^2\Delta$  and  $1^4\Pi$  states of BAr and the spin-orbit interactions that couple these states. It will emerge that a careful analysis of the spin-orbit interaction provides key insights into the novel nature of the bonding in the  $C^2\Delta$  state, insights that can be generalized to both, other states in BAr, and more significantly, to other open shell van der Waals complexes. The dynamics of the predissociation of the  $C^2\Delta$  state will be considered in detail in a forthcoming pair of complementary experimental and theoretical studies.<sup>9,8</sup>

Section II presents our theoretical description of the  $C^2\Delta$  and  $1^4\Pi$  states of BAr. The  $C^2\Delta$  state turns out to be surprisingly difficult to describe. A principal concern is that the reliability of the calculation should be uniform with respect to molecular geometries so that the potential energy curves have the proper shape. In order to accomplish this, the computational approach to the treatment of electron correlation and the atomic orbital basis sets must be equally valid for each of the electronically excited states in question in both the atomic and molecular regions. An excellent review of computational approaches for

electronically excited states has been given by Bruna and Peyerimhoff.<sup>10</sup> Bauschlicher and Langhoff have reviewed the application of these methods to molecular spectroscopy.<sup>11</sup> Much effort has been expended designing basis sets for molecular calculations. These developments, however, tend to focus on the electronic ground state.<sup>12</sup> Detailed basis set studies, like that of Fülcher and Roos for excited states in pyrazine<sup>13</sup> or that of Kendall, Dunning, and Harrison<sup>14</sup> for atomic anions, are infrequent.

In section III we present the results of a systematic treatment of  $B(2^2D, 4P)$  and  $BAr(1^4\Pi, C^2\Delta)$ . A proper description of these excited states requires careful tuning of the basis set to accommodate a near degeneracy of valence  $2s2p^2$ , and Rydberg  $2s^23d$   $2D$  boron terms. Also considered is the effect of the level of electron correlation on the potential energy curves for the excited  $C^2\Delta$  and  $1^4\Pi$  states. It is found that high-order electron correlation is required to describe accurately the unusually strong binding in  $BAr(C^2\Delta)$ . The  $1^4\Pi \sim C^2\Delta$  spin-orbit coupling is also reported and discussed in terms of the single-configuration picture. This analysis offers insights into the heavy atom effect on the fine-structure splitting of the  $2^2\Pi_{\Omega}$  manifold for the van der Waals molecules  $M(np)Rg$ , where  $M = Li, Na$  and  $Rg = Ne, Ar, Kr$ . A careful analysis of the wave function for the  $C^2\Delta$  state, guided by the geometry dependence of the spin-orbit interaction, reveals that the bonding in the  $C^2\Delta$  state can be understood, in terms of a simple molecular orbital picture, as a type of coordinate covalency, dative bonding, with the total binding extremely sensitive to the level of electron correlation. This suggestion was confirmed by explicit calculation. Our analysis suggests, and preliminary calculations confirm, that the  $1^4\Sigma^-$  state, which differs from the  $C^2\Delta$  state in the molecular region only by a spin recoupling, should be bound.

Section IV summarizes and suggests directions for future investigation.

## II. Theoretical Approach

**A. Qualitative Description of the Electronic Structure of BAr.** The low-lying electronic states of BAr arise from ground-state atomic argon,  $Ar(1S)$  in combination with different electronic states of atomic boron, see Figure 1. The energies of these states at the separated atom limit correspond to the degeneracy-weighted averages of the atomic levels composing a given term. The degeneracy-weighted averages are<sup>15</sup>  $E(2s^2-2p^2P) = 10.169 \text{ cm}^{-1}$ ,  $E(2s2p^2 4P) = 28877 \text{ cm}^{-1}$ ,  $E(2s^23s^2S)$

<sup>‡</sup> Supported by AFOSR Grant F49620-96-1-0017.

<sup>⊗</sup> Abstract published in *Advance ACS Abstracts*, April 1, 1997.

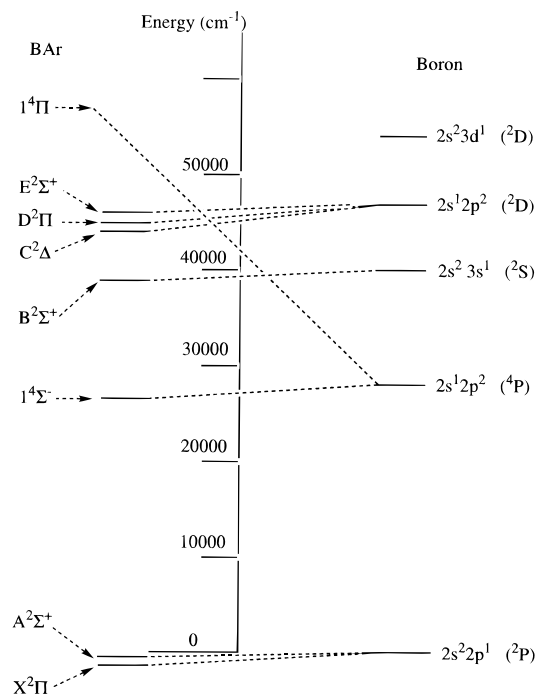


**Figure 1.** Correlation diagram for BAr. Note that the binding energies in BAr  $X^2\Pi$ ,  $A^2\Sigma^+$ ,  $B^2\Sigma^+$ ,  $D^2\Pi$ , and  $E^2\Sigma^+$  have been exaggerated to emphasize that they are bound states.

$= 40039 \text{ cm}^{-1}$ , and  $E(2s^2p^2 \ ^2D) = 47857 \text{ cm}^{-1}$ . Figure 1 illustrates the following: (i) The ground state  $1s^22s^22p^1 \ ^2P$  term splits into the very weakly bound  $X^2\Pi$  ground state and the  $A^2\Sigma^+$  state. (ii) The  $1s^22s^12p^2 \ ^4P$  term splits into the  $1^4\Sigma^-$  and the  $1^4\Pi$  states, while the higher energy  $1s^22s^12p^2 \ ^2D$  term splits into the bound  $C^2\Delta$  state as well as a  $^2\Pi$  state and a  $^2\Sigma^+$  state, both of which lie above the  $C^2\Delta$  state in energy. (iii) Between the valence  $1s^22s^12p^2 \ ^4P$  and  $^2D$  asymptotes lies a  $1s^22s^23s^1 \ ^2S$  Rydberg asymptote. This term gives rise to the weakly bound  $B^2\Sigma^+$  molecular state. (iv) Particularly relevant in the present context is the nominally Rydberg  $1s^22s^23d^1 \ ^2D$  term at  $54767 \text{ cm}^{-1}$ , only  $6910 \text{ cm}^{-1}$  higher in energy than the nominal valence  $1s^22s^12p^2 \ ^2D$  term. As a result valence–Rydberg mixing is important for the correct description of the  $^2D$  term at  $47857 \text{ cm}^{-1}$ , a fact which has important implications in designing a basis set appropriate for describing the excited  $C^2\Delta$  state.

**B. Computational Methods.** Multireference configuration-interaction (MRCI)<sup>16</sup> wave functions based on molecular orbitals determined from a state-averaged multiconfigurational self-consistent field<sup>17–19</sup> (SA-MCSCF) procedure are employed in this work. This level of treatment is dictated by the multireference character of the  $C^2\Delta$  state and the necessity of having exact eigenfunctions of  $S^2$  for the calculation of the interstate spin–orbit interaction.

Because BAr is a weakly interacting molecule, the molecular orbitals are only slightly perturbed from their atomic orbital counterparts and therefore the most convenient labeling of the molecular orbitals is by their dominant atomic orbital component denoted as Ar  $1s$ ,  $2s$ ,  $2p_x$ ,  $2p_y$ , etc. and B  $1s$ ,  $2s$ ,  $2p_x$ , etc.

*i. Atomic Orbital Basis Sets.* Six different basis sets were used in this study, denoted AVDZ, TZ0F, TZ1F, AVTZ, AVTZ-(4d), and AVTZ(5d), listed here in approximate order of increasing completeness.

(a) The AVDZ basis set is an augmented valence double-zeta set used in a previous study of BAr by Alexander,<sup>20,21</sup> which was derived from the correlation-consistent augmented valence double-zeta basis of Dunning.<sup>22</sup> It consists of Ar( $13s/9p/2d$ )

and B( $10s/5p/2d$ ), contracted to Ar( $5s/4p/2d$ ) and B( $4s/3p/2d$ ), respectively.

(b) The AVTZ basis set is an augmented valence triple-zeta basis set, also used in a previous study of BAr by Alexander,<sup>20,21</sup> which was derived from the correlation-consistent augmented valence triple-zeta basis of Dunning.<sup>22</sup> It consists of Ar( $16s/10p/3d/2f$ ) and B( $11s/6p/3d/2f$ ) contracted to Ar( $6s/5p/3d/2f$ ) and B( $5s/4p/3d/2f$ ), respectively.

The remaining triple-zeta sets were obtained from the AVTZ set as follows:

(c) AVTZ(4d): A fourth d-function (exponent 0.0185) was added to boron in the AVTZ basis to yield Ar( $6s/5p/3d/2f$ ) and B( $5s/4p/4d/2f$ ).

(d) AVTZ(5d): A fifth d-function (exponent 0.0057) was added to boron in the AVTZ(4d) basis to yield Ar( $6s/5p/3d/2f$ ) and B( $5s/4p/5d/2f$ ).

(e) TZ0F: All f-functions were dropped from AVTZ(4d).

(f) TZ1F: An f-function (exponent 0.163) was added to boron in the TZ0F basis to yield Ar( $6s/5p/3d$ ) and B( $5s/4p/4d/1f$ ).

Cartesian Gaussian functions ( $1 \times s$ ,  $3 \times p$ ,  $6 \times d$ ,  $10 \times f$ ) were employed so the total number of basis functions in each case is: AVDZ = 54, TZ0F = 80, TZ1F = 90, AVTZ = 114, AVTZ(4d) = 120, and AVTZ(5d) = 126. The new d-function exponents for AVTZ(4d) and AVTZ(5d) were generated in an even-tempered manner<sup>23</sup> based on the existing d-exponents in the AVTZ basis set.

*ii. Configuration Interaction Treatment.* For the configuration interaction (CI) calculations, except where otherwise noted, the orbital space was partitioned as follows: The core space consisted of the Ar  $1s$ ,  $2s$ ,  $2p_{x,y,z}$ ,  $3s$ , and B  $1s$  orbitals. The active space consisted of the Ar  $3p_{x,y,z}$ , and B  $2s$ ,  $2p_{x,y,z}$ , and  $3d_{xy}$  orbitals. All remaining orbitals were taken to form the virtual space. It was computationally expedient to exclude the B  $3d_{x^2-y^2}$  orbital from the active space because only the  $^2\Delta_{xy}$  component of the  $C^2\Delta$  state was treated. This orbital partitioning was also used in the SA-MCSCF procedure except that the Ar  $3p_{x,y,z}$  orbitals were included the core orbital space.

It is particularly crucial to include the Ar  $3p_z$  orbital in the active space of the CI calculations since correlation of this orbital contributes heavily to the bonding in the  $C^2\Delta$  state. If *only* the Ar  $3p_z$  orbital is removed from the active space, the  $C^2\Delta$  state is predicted to be *essentially unbound*, whereas its true well depth is  $\sim 3700 \text{ cm}^{-1}$ .<sup>8</sup> This observation is important for our interpretation of the bonding in BAr( $C^2\Delta$ ). On the other hand, inclusion of the Ar  $3p_z$  orbital in the active space of the SA-MCSCF treatment has little effect at the CI level. The effects of electron correlation in the description of the  $C^2\Delta$  state will be discussed in greater detail in section III.

For the atomic boron calculations, an equivalent partitioning of orbital space was used. The B  $1s$  orbital was taken as the core space, and the B  $2s$ ,  $2p_{x,y,z}$ , and  $3d_{xy}$  orbitals were taken as the active space. All remaining orbitals were taken as virtual orbitals.

Calculations are reported at three levels, first-order CI (FOCI),<sup>24</sup> second-order CI (SOCI),<sup>24</sup> and second-order CI with the Davidson correction (SOCI+DC). The multireference version of the Davidson correction.<sup>25–27</sup> was employed to approximate the contribution of quadruple excitations. In these calculations, the sum of the weights of the reference configurations ( $\sum_i c_i^2$ ) was always greater than 0.91. Table 1 shows the number of configuration state functions (CSFs)<sup>16</sup> in the SOCI expansion for each of the basis sets used. For the molecular calculations the computational expense of the SOCI/AVTZ(4d) treatment, using method/basis notation, was prohibitive due to

**TABLE 1: Number of CSFs in the SOCI/basis Expansion<sup>a</sup>**

basis	boron		
	<sup>2</sup> P	<sup>4</sup> P	<sup>2</sup> D
AVDZ	577	267	538
AVTZ	3317	1602	3165
TZ0F	1746	836	1654
TZ1F	2815	1358	2677
AVTZ(4d)	4132	2004	3948
AVTZ(5d)	5035	2450	4819

basis	BAr		
	X <sup>2</sup> Π	1 <sup>4</sup> Π	C <sup>2</sup> Δ
AVDZ	1 184 008	1 017 066	1 183 304
TZ0F	3 250 588	2 805 216	3 248 940
TZ1F	4 317 608	3 729 486	4 315 672
AVTZ(4d)	8 425 868	7 290 696	8 422 972

<sup>a</sup> BAr SOCI/AVTZ(4d) calculations were not performed.

the large size of the CSF expansion. The number of CSFs in that case is shown merely for purposes of comparison.

*iii. Molecular Orbitals: State-Averaged MCSCF.* The molecular orbitals used in both the atomic boron and BAr CI treatments were obtained from SA-MCSCF calculations. In the molecular calculations, the X<sup>2</sup>Π ground state, the repulsive 1<sup>4</sup>Π state, and the C<sup>2</sup>Δ state were averaged. Considered in the atomic calculations were the corresponding components of the <sup>2</sup>P, <sup>4</sup>P, and <sup>2</sup>D states. The weight vector used was  $\mathbf{w} = (1,1,2)$ . The sensitivity of the energetics to changes in the weight vector was investigated. At the SOCI level, with the AVDZ basis, changing the weight vector to  $\mathbf{w} = (1,1,6)$  and later to  $\mathbf{w} = (1,1,20)$  produced changes in the differences in energy among the states typically on the order of a few tens of cm<sup>-1</sup> and changed the binding energy of the C<sup>2</sup>Δ state by at most 82 cm<sup>-1</sup>. These changes were judged sufficiently minor to warrant no further attention, and the weight vector  $\mathbf{w} = (1,1,2)$  was used in all subsequent atomic and molecular calculations.

### III. Results and Discussion

**A. Atomic Calculations.** The results at the Ar + B asymptote provide a useful guide to the accuracy of the present treatment. Calculations are reported for the ground <sup>2</sup>P and excited <sup>4</sup>P and <sup>2</sup>D terms of atomic boron with the six different basis sets and the three levels of CI. The convergence of  $E(Z)$ , the energy of the Z term, with basis set is shown in Figure 2. The variations in  $E(^2P)$  and  $E(^4P)$  with basis set are qualitatively very similar and quite different from that of  $E(^2D)$ . The most important difference is in the addition of extra d-functions. While the  $E(^4P)$  are already converged at the AVTZ level with respect to the addition of more diffuse d-functions to the orbital basis, the addition of a fourth d-function, AVTZ → AVTZ(4d), is required to reach convergence for the <sup>2</sup>D energy. The effect of adding a fifth d-function, AVTZ(4d) → AVTZ(5d), is virtually nil. The diffuse d-character is a consequence of the quasi degenerate 1s<sup>2</sup>2s<sup>2</sup>3d<sup>1</sup> <sup>2</sup>D electron configuration which contributes ~18% ( $c_i^2 \approx 0.18$ ,  $i = 1s^2 2s^2 3d_{xy}$ ) to the lowest <sup>2</sup>D term.

Thus because of the Rydberg d-character in the nominal B 1s<sup>2</sup>2s<sup>1</sup>2p<sup>2</sup> <sup>2</sup>D term, it is necessary to extend the AVTZ basis with extra diffuse d-functions, even though this basis is quite adequate for the 1s<sup>2</sup>2s<sup>1</sup>2p<sup>2</sup> <sup>2</sup>P, <sup>4</sup>P terms. Bruna and Peyerimhoff<sup>10</sup> have discussed this need to add such "spectroscopic" orbitals to achieve a proper description of excited states having Rydberg character. See also the treatment of excited states of BeC by Wright and Kolbuszewski<sup>28</sup> and the relativistic calculations on ground- and excited-state LiHg by Gleichmann and Hess.<sup>29</sup>

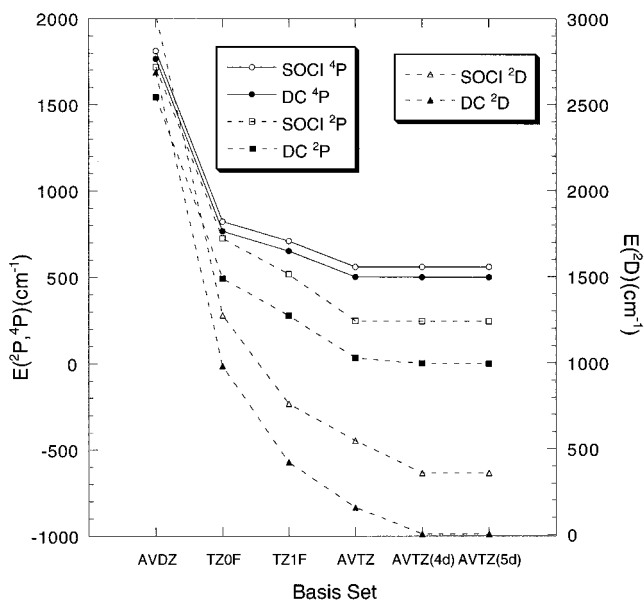


**Figure 2.** Convergence of the ground 1s<sup>2</sup>2s<sup>2</sup>2p<sup>1</sup> <sup>2</sup>P and excited 1s<sup>2</sup>2s<sup>1</sup>2p<sup>2</sup> <sup>4</sup>P states, left hand ordinate, and the 1s<sup>2</sup>2s<sup>1</sup>2p<sup>2</sup> <sup>2</sup>D excited state, right hand ordinate, of boron with respect to basis set for two levels of CI. Solid lines with circular marker represent <sup>2</sup>P, broken lines with square marker <sup>4</sup>P, and broken lines with triangular marker <sup>2</sup>D. In all cases the open marker represents SOCI and filled marker SOCI+DC. Note that a fourth d-function is required to accurately describe the <sup>2</sup>D state. This is due to the contribution of the Rydberg 1s<sup>2</sup>2s<sup>2</sup>3d<sup>1</sup> <sup>2</sup>D configuration which nominally describes a term just 6910 cm<sup>-1</sup> higher in energy. SOCI+DC/AVTZ(5d) results translated for clarity. Energies at the SOCI+DC/AVTZ(5d) level are  $E(^2P) = -24.600\,205$  au,  $E(^4P) = -24.467\,985$  au, and  $E(^2D) = -24.381\,894$  au. The line segments joining the markers are drawn as a visual aid and are not intended to suggest interpolation.

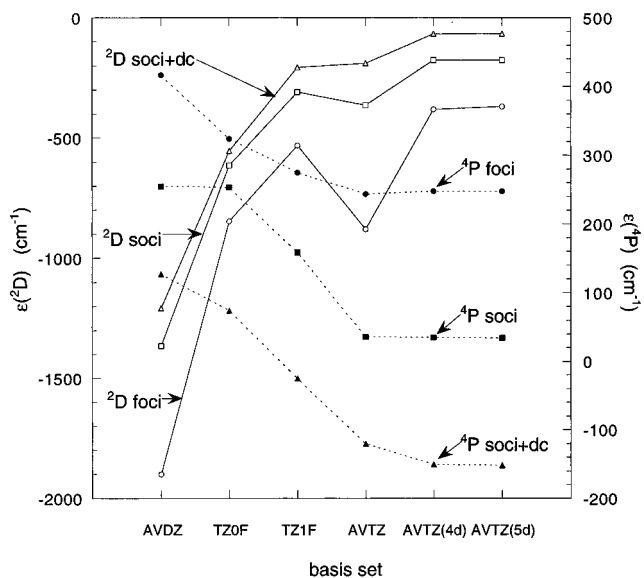


**Figure 3.** Errors in the computed separations of the states of atomic boron for six basis sets and three levels of CI. Broken lines with solid markers show  $\epsilon(^4P)$ ; solid lines with open markers show  $\epsilon(^2D)$ . The line segments joining the markers are drawn as a visual aid and are not intended to suggest interpolation.

It is also enlightening consider the atomic term separations,  $\Delta E(X) \equiv E(X) - E(^2P)$ , computed with different levels of electron correlation. Figure 3 shows the error in  $\Delta E(X)$ ,  $\epsilon(X) \equiv \Delta E(X) - \Delta E_{\text{exp}}(X)$ , for  $X = ^4P$  and <sup>2</sup>D calculated with the six different basis sets and the three levels of CI. Here  $\Delta E_{\text{exp}}(X)$  refers to  $\Delta E(X)$  derived from experimental data.<sup>30</sup> Two features deserve special mention. First, note that  $\epsilon(^2D)$  is typically much

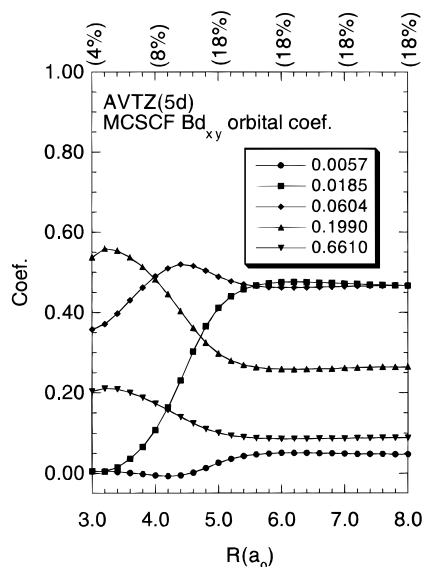


**Figure 4.** Coefficient of each B  $d_{xy}$ -function in the SA-MCSCF description of the  $1\delta_{xy}$  orbital (nominally B  $3d_{xy}$ ) as a function of internuclear separation. Note the increasing importance of the diffuse functions at large  $R$ . The figures given parenthetically adjacent to the upper horizontal axis indicate  $c_i^2$  of the ...  $\sigma^2\delta_{xy}$  CSF in the MCSCF expansion for the  $C^2\Delta$  state.

larger than  $\epsilon(^4P)$ . Again we see that the AVDZ and AVTZ basis sets, designed for ground-state calculations, are much less adequate for describing nominally  $1s^22s^12p^2\ ^2D$  boron. Second, note that  $\epsilon(^2D)$  obtained with the AVTZ basis is comparable or actually worse than that obtained with TZ1F basis, although the AVTZ basis is larger. This is because the extra functions in the AVTZ basis are f-functions and, as shown above, a proper description of nominally  $1s^22s^12p^2\ ^2D$  boron requires extra diffuse d-functions.  $\epsilon(^2D)$  improves considerably in going from AVTZ to AVTZ(4d). The TZ1F basis represents a compromise basis which is augmented with a set of d-functions but includes only a single set of f-functions. This improves computational efficiency by reducing the total number of functions and improves the accuracy with which B  $^2D$  is described, while sacrificing little in the accuracy of the description of B  $^2P$  and  $^4P$ .

This analysis provides a clear picture of the level of treatment needed to ensure a proper description of the B + Ar asymptote and suggests TZ1F as the basis of choice for the molecular calculations. The SOCI/TZ1F wave functions will be used to compute the  $1^4\Pi$ - $C^2\Delta$  spin-orbit interaction

$$H^{SO}(1^4\Pi, C^2\Delta) \equiv i\langle\Psi_{1^4\Pi_x(3/2)}|H^{SO}|\Psi_{C^2\Delta_{xy}(1/2)}\rangle \quad (1)$$

where  $M_s$  is given parenthetically, and  $H^{SO}$  is the full Breit-Pauli spin-orbit Hamiltonian including the one-electron spin-orbit and the two-electron spin-other-orbit contributions.<sup>31</sup> These results will be compared with those at the FOCI/AVDZ and SOCI/AVDZ levels.

**B. Molecular Calculations.** We begin by considering the geometry dependence of the valence-Rydberg mixing in the  $C^2\Delta$  state. This issue is addressed in Figure 4 which shows the relative contributions of the five d-functions in the AVTZ-(5d) basis set in the MCSCF description of the  $C^2\Delta$  state and also reports the percent Rydberg character, the square of the coefficient of the CSF corresponding to  $B(1s^22s^23d_{xy})$ . Note that at large separations, the fourth d-function (exponent 0.0185) contributes heavily to the description of the  $C^2\Delta$  state. The fifth d-function (exponent 0.0057), however, contributes very

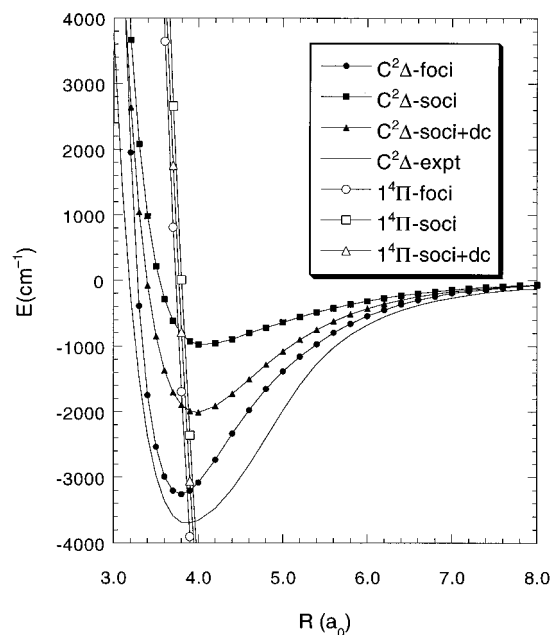


**Figure 5.** Potential energy curves for the  $1^4\Pi$  (open markers) and  $C^2\Delta$  (solid markers) states of BAR at (FOCI, SOCI, SOCI-DC)/TZ1F levels. The experimentally deduced potential energy curve for the  $C^2\Delta$  state was given by Yang and Dagdigian.<sup>8</sup> The asymptotes have been set equal to the experimental separation for purposes of comparison. little at any geometry, confirming the adequacy of the AVTZ-(4d) basis. Note too the Rydberg character decreases with decreasing B-Ar distance,  $R$ , such that in the molecular region the  $C^2\Delta$  state is predominantly valence (92%) in character. However the correct description of valence-Rydberg mixing is essential for the description of the  $C^2\Delta$  potential energy curve for internuclear separation,  $R$ , greater than  $4.5a_0$ . This portion of the  $C^2\Delta$  potential energy curve is key to the description of the  $\text{BAr}(C^2\Delta, \nu > 12)$  levels, whose radiationless decay provided the motivation for the present study. See refs 8 and 9.

Figure 5 reports the potential energy curves for the  $C^2\Delta$  and  $1^4\Pi$  states,  $E_{C^2\Delta}(R)$  and  $E_{1^4\Pi}(R)$ , at the FOCI, SOCI, and SOCI+DC levels using the TZ1F basis and compares the result with  $E_{C^2\Delta}(R)$  inferred from an experiment that recorded  $C^2\Delta, \nu = 13-17$ .<sup>8</sup> Note that the form of  $E_{1^4\Pi}(R)$  differs little at the FOCI, SOCI, and SOCI+DC levels and that the  $1^4\Pi$ - $C^2\Delta$  crossing point,  $R_x$ , occurs in the immediate vicinity of equilibrium geometry,  $R_e(C^2\Delta)$ , at all levels of theory. This has important implications for  $C^2\Delta$  predissociation as discussed in refs 8 and 9.

Our best estimate of  $R_e = 3.99a_0$  (SOCI+DC/TZ1F) is in excellent agreement with the experimental value of  $R_e = 3.97a_0$ .<sup>8</sup> The well depth for the  $C^2\Delta$  state,  $D_e(C^2\Delta)$ , proved to be quite sensitive to the level of treatment. The FOCI/TZ1F value,  $D_e(C^2\Delta) = 3187$  (3700)  $\text{cm}^{-1}$ , is reasonably close to the value inferred from the experimental measurements,<sup>8</sup> shown parenthetically. This agreement is fortuitous since the result is not converged with respect to the level of treatment. The SOCI value is too small and in much poorer agreement with experiment than the FOCI value. The SOCI+DC treatment improves  $D_e$  considerably to 2015  $\text{cm}^{-1}$ , although this result is still in error by a factor of 1.83 compared to the experimental value. Some improvement could be expected by using a more complete atomic orbital basis. At the FOCI level, improving the orbital basis from TZ1F to AVTZ(4d) resulted in only a 17% improvement in  $D_e(C^2\Delta)$ . It appears therefore that a high-order multireference configuration-interaction treatment will be necessary to accurately reproduce  $D_e(C^2\Delta)$ . This discrepancy is not entirely unexpected. A similar discrepancy was found

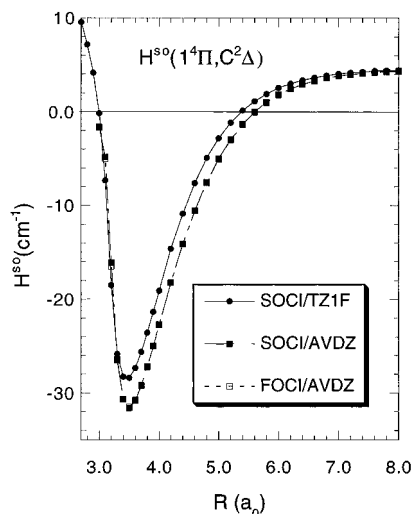


**Figure 6.** Spin-orbit coupling of BAr  $1^4\Pi$  and  $C^2\Delta$ ,  $H^{SO}(1^4\Pi, C^2\Delta)$ .

by Hwang et al. in their treatment of bonding in BAr( $B^2\Sigma^+$ ).<sup>32</sup> These authors reported a best theoretical  $D_e$  of  $455\text{cm}^{-1}$  compared with the experimental  $D_e$  of more than twice that value, approximately  $1100\text{cm}^{-1}$ . Below we will note that the observed discrepancies are in fact consistent with the suggested origin of the bonding.

Note that a method that ignored the near degeneracy effect at the asymptote, such as the popular coupled cluster approaches,<sup>33</sup> would be expected to obtain a fortuitously improved  $D_e(C^2\Delta)$  but at the expense of correctly describing the relative separation of the  $^2D$  and  $^4P$  asymptotes.

Figure 6 reports the  $C^2\Delta-1^4\Pi$  spin-orbit interaction,  $H^{SO}(1^4\Pi, C^2\Delta)$ , at the FOCI/AVDZ, SOCI/AVDZ, and SOCI/TZ1F levels. It is important to observe that the FOCI/AVDZ and SOCI/AVDZ results are virtually indistinguishable and these results differ little from the SOCI/TZ1F values.

When considering the binding of van der Waals molecules the issue, of basis set superposition error (BSSE) should be addressed. While methods exist for evaluating the magnitude of the BSSE, such as the counterpoise correction of Boys and Bernardi,<sup>34</sup> they are unwieldy to apply in MRCI calculations.<sup>32</sup> It is unlikely given the size of  $D_e$  and the extended nature of the basis set used here that BSSE would be a serious problem. This is supported by the work by Hwang et al.<sup>21</sup> who report calculations for the  $X^2\Pi$ ,  $A^2\Sigma^+$ , and  $B^2\Sigma^+$  states of BAr using comparable basis sets. They report a BSSE of  $14.3\text{cm}^{-1}$  for the  $X^2\Pi$  state,  $16.1\text{cm}^{-1}$  for the  $A^2\Sigma^+$  state, and  $80.4\text{cm}^{-1}$  for the  $B^2\Sigma^+$  state.

As noted previously, a multireference description is used for the characterization of the  $C^2\Delta$  state. Our use of a multireference CI method raises the issue of the effect of the lack of size consistency. In fact, the development of size-consistent MRCI techniques is an active area of research.<sup>35,36</sup> The size-consistency error is given as<sup>21</sup>

$$\epsilon_{SC}(X) = E_{BAr(M)}(\infty) - E_{Ar(1S)} - E_{B(X)} \quad (2)$$

where  $M(R) \rightarrow Ar(1S) + B(X)$  as  $R \rightarrow \infty$ . Of principal concern, the size-consistency error in the separation  $E(^2D) - E(^4P)$ , is given by

$$\Delta\epsilon_{SC}(^2D) = \epsilon_{SC}(^2D) - \epsilon_{SC}(^4P) = [E_{BAr, C^2\Delta}(\infty) - E_{BAr, 1^4\Pi}(\infty)] - [E_{B, ^2D} - E_{B, ^4P}] \quad (3)$$

With the TZ1F basis set the value of  $\Delta\epsilon_{SC}(^2D)$  is  $739\text{cm}^{-1}$  at the SOCI level and  $209\text{cm}^{-1}$  at the SOCI+DC level. The

Davidson correction makes a 3.5-fold reduction in the size-consistency error. Note, however, that the size-consistency error is just 10% of the predicted  $2000\text{cm}^{-1}$  binding energy of the  $C^2\Delta$  state.

**C. The Origin of the  $C^2\Delta$  Bonding.** Although strong binding in van der Waals molecules is not unknown,<sup>4,37,38</sup>  $D_e(C^2\Delta)$  is remarkably large for a van der Waals molecule, so it is important to consider the origin of the bonding.

In open shell van der Waals species (ARg), strong binding may be attributable to Rydberg character in the molecular state<sup>28</sup> which facilitates an ion-induced dipole interaction of the  $A^+$  core with the Rg atom. This Rydberg shell penetration model has been successfully invoked in the case of AlAr<sup>39</sup> and HgAr.<sup>40</sup> In a similar vein, Massick and Breckenridge<sup>37,38</sup> have reported a strongly bound doubly excited valence state, the  $^3\Sigma^-$  state, of the neutral van der Waals molecule Mg( $3p_\pi^2$ )Ar. They suggest that the absence of occupied Mg  $3s$ ,  $3p_z$  orbitals and the perpendicular orientation of the Mg  $3p_\pi$  orbitals permit the Ar to approach the  $Mg^{2+}$  core. This results in an Ar-Mg<sup>2+</sup> ion-induced dipole attraction as above as, as well as a dispersive Mg( $3p_\pi$ )-Ar( $3p_\pi$ ) attraction. On the other hand, Hwang et al.<sup>21</sup> have reported strong binding for the  $B^2\Sigma^+$  state of BAr which is Rydberg in character. These authors considered the possibility that the strong binding might arise from the ion-induced dipole interaction of the  $B^+$  core with the Ar atom—once the Ar has penetrated inside the B  $3s$  Rydberg shell. They, however, argued against the Rydberg shell penetration model as an explanation for the strong bonding, citing the lack of bonding at levels of theory involving little electronic correlation. They concluded that the bonding in the  $B^2\Sigma^+$  state results from a delicate interaction of electron correlation and polarization which defies a simple chemical description. Similarly Esposti and Werner<sup>41</sup> noted that bonding in the A state of the ArOH van der Waals molecule arises predominantly from electronic correlation effects and that simple molecular orbital descriptions are inadequate.

Since the Rydberg character of the  $C^2\Delta$  state decreases as the bond distance decreases, the Rydberg-based core penetration model cannot be operative here. Instead, an alternative explanation of the bonding in BAr( $C^2\Delta$ ) is offered which, although quite distinct from, involves some of the ideas used in the Breckenridge approach noted above.<sup>4,37</sup>

*i. Analysis of the Spin-Orbit Interaction.* A clue to the origin of the bonding in the  $C^2\Delta$  state is found in the  $C^2\Delta-1^4\Pi$  spin-orbit interaction pictured in Figure 6. Consider the region near  $R_e(C^2\Delta)$  where the spin-orbit interaction changes dramatically. The  $C^2\Delta$  and  $1^4\Pi$  states are dominated by the following CSFs

$$\begin{aligned} \Psi_{1^4\Pi_x} &= \dots 2\pi^4 6\sigma^2 7\sigma\alpha 3\pi_x \alpha 8\sigma\alpha \\ \Psi_{C^2\Delta_y} &= \dots 2\pi^4 6\sigma^2 7\sigma\alpha (3\pi_x 3\pi_y) (\alpha\beta - \beta\alpha) \end{aligned} \quad (4)$$

where the  $6\sigma$ ,  $2\pi$ ,  $7\sigma$ ,  $8\sigma$ , and  $3\pi$  orbitals asymptotically have Ar  $3p_z$ , Ar  $3p_\pi$ , B  $2s$ , B  $2p_z$ , and B  $2p_\pi$  character, respectively. In the popular one-electron approximation to the spin-orbit operator the  $1^4\Pi \sim C^2\Delta$  spin-orbit interaction given by

$$H^{SO}(1^4\Pi, C^2\Delta) \approx \langle 8\sigma | h_x^{SO} | 3\pi_y \rangle \quad (5)$$

where  $h_x^{SO}$  is the  $x$ -component of the spatial part of the real-valued spin-orbit operator.<sup>31</sup> This matrix element is antihermitian.<sup>31</sup>

Figure 7 shows the leading atomic orbital contributions to the  $8\sigma$  orbital. This orbital, a B  $2p_z$  orbital for large  $R$ ,  $s-p$

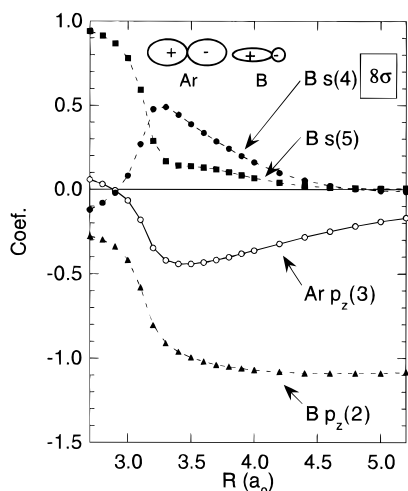


**Figure 7.** Dominant atomic orbital contributions to the  $8\sigma$  molecular orbital of BAr (nominally B  $2s-2p_z$ ) determined from the SA-MCSCF procedure, as a function of internuclear separation,  $R$ . A picture of the orbital arrangement (for  $R$  small but greater than  $R_c$ ) is included.

hybridizes and gains Ar  $3p_z$  character in an antibonding manner as  $R$  decreases. For the smallest  $R$  in Figure 7, its character changes as it acquires diffuse B  $s$ , Rydberg, character. The  $3\pi$  orbital similarly acquires Ar  $3p_\pi$  character, again in an antibonding manner, but unlike the  $8\sigma$  orbital, the Ar contribution does not change character over the range considered.

From eq 5 the  $R$  dependence of  $H^{SO}(1^4\Pi, C^2\Delta)$  in Figure 6 can be understood from the  $R$  dependence of the  $3\pi$  and the  $8\sigma$  orbitals which from the above discussion have qualitatively the form

$$8\sigma(R) = s_1(R) B(2p_z) + s_2(R) Ar(3p_z) \quad (6a)$$

$$3\pi_y(R) = p_1(R) B(2p_y) - p_2(R) Ar(3p_y) \quad (6b)$$

so that

$$H^{SO}(1^4\Pi, C^2\Delta) \approx s_1(R)p_1(R)\langle B_{2p_z} | h_x^{SO} | B_{2p_y} \rangle - s_2(R)p_2(R)\langle Ar_{3p_z} | h_x^{SO} | Ar_{3p_y} \rangle \quad (7)$$

Here the often used single-center approximation to the spin-orbit operator is invoked. The first integral in eq 7 is expected to be much smaller than the second, owing to the differences in the boron<sup>15</sup> and argon cation<sup>30</sup> spin-orbit coupling constants,  $\xi_B = 10.160 \text{ cm}^{-1}$  and  $\xi_{Ar^+} = -954.7 \text{ cm}^{-1}$ . As noted below however, both integrals in eq 7 are expected to have the same sign. Note too that for the smallest  $R$  considered, in the region of the repulsive wall of the  $C^2\Delta$  state, this model breaks down although the computed results remain reliable.

The origin of the  $R$  dependence of  $H^{SO}(1^4\Pi, C^2\Delta)$  in Figure 6 is now clear. At large  $R$ ,  $|s_1|$  and  $|p_1|$  are large and  $|s_2|$  and  $|p_2|$  are small; see Figure 7. The boron contribution to the spin-orbit coupling dominates, and the value of  $H^{SO}(1^4\Pi, C^2\Delta)$  is close to the atomic boron limit. As  $R$  decreases,  $|s_2|$  and  $|p_2|$  increase and there is a contribution from the argon-centered spin-orbit interaction. This is the external heavy atom effect. Note that as this simple model indicates, both the  $8\sigma$  and  $3\pi$  orbitals must acquire Ar character for the heavy atom effect to be observed in  $H^{SO}(1^4\Pi, C^2\Delta)$ . Figure 6 clearly shows  $H^{SO}(1^4\Pi, C^2\Delta)$  being overtaken by the Ar contribution with decreasing  $R$ , changing sign when the Ar contribution exceeds the B contribution, and peaking around  $R = 3.5a_0$ , where the Ar( $3p_z$ ) contribution to the  $8\sigma$  orbital reaches its maximum; see Figure

7. For  $R < 3.5a_0$ , the Ar contribution to the  $8\sigma$  orbital drops rapidly and then changes sign. This change in orbital character is also reflected in  $H^{SO}(1^4\Pi, C^2\Delta)(R)$ . Thus the marked  $R$  dependence of  $H^{SO}$  is seen to be consequence of the external heavy atom effect.

Although somewhat tangential to this work, the preceding analysis can be used to consider the geometry dependence of the fine-structure splitting in the  $C^2\Delta_\Omega$  and the  $1^4\Pi_\Omega$  manifolds. The fine-structure splitting for the  $C^2\Delta$  state is given by

$$\Delta_{C^2\Delta}(R) = E_{C^2\Delta_{5/2}}(R) - E_{C^2\Delta_{3/2}}(R) = 2i\langle \Psi_{C^2\Delta_{xy}(1/2)} | H^{SO} | \Psi_{C^2\Delta(x^2-y^2)(1/2)} \rangle \quad (8a)$$

while for the  $1^4\Pi_\Omega$  manifold, which has components  $\Omega = 5/2, 3/2, 1/2, 1/2$ , we use, to emphasize the analogy with eq 8a, the  $4^1\Pi_{5/2}$  state and, the  $4^1\Pi_{1/2}$  state given at zeroth order by  $4^1\Pi^-(3/2)$ , so that

$$\Delta_{1^4\Pi}(R) = E_{1^4\Pi_{5/2}}(R) - E_{1^4\Pi_{1/2}}(R) = 2i\langle \Psi_{1^4\Pi_y(3/2)} | H^{SO} | \Psi_{1^4\Pi_x(3/2)} \rangle \quad (8b)$$

At the single configuration approximation given in eq 4 the two components of the  $C^2\Delta$  wave function represent a  $\sigma$  electron coupled to the two components of a  $\pi^2(^1\Delta)$  shell. As a consequence  $\Delta_{C^2\Delta} \approx 0$ , independent of the detailed form of the molecular orbitals in eq 4, that is, for all  $R$ . On the other hand, for  $1^4\Pi$  we have

$$\Delta_{1^4\Pi}(R) \approx \langle 3\pi_y | h_z^{SO} | 3\pi_x \rangle \approx p_1(R)^2 \langle B_{2p_y} | h_z^{SO} | B_{2p_x} \rangle + p_2(R)^2 \langle Ar_{3p_y} | h_z^{SO} | Ar_{3p_x} \rangle \quad (8c)$$

Thus unlike  $\Delta_{C^2\Delta}(R)$ ,  $\Delta_{1^4\Pi}(R)$  is expected to increase as  $R$  decreases because of the contribution of the second term in eq 8c. However  $\Delta_{1^4\Pi}(R)$  is not expected to change sign as  $R$  decreases since the two integrals in eq 8c have the same sign. This might seem counterintuitive since  $Ar^+(2P)$  is inverted while  $B(2P)$  is regular. However it is in fact correct. The change from regular to inverted fine-structure splittings (for states dominated by a single CSF) is a consequence of the antisymmetric nature of the electronic wave function. In this regard compare the fine-structure splitting of a  $2^1\Pi$  state corresponding to the CSFs  $\pi_x\alpha, \pi_y\alpha$ , that is a  $\pi^1$  electron configuration, with that of a  $2^1\Pi$  state corresponding to the CSFs  $\pi_x\alpha\pi_y^2, \pi_x^2\pi_y\alpha$ , that is a  $\pi^3$  electron configuration, using the same set of orbitals. The fine-structure splitting,  $E^2\Pi_{3/2}(R) - E^2\Pi_{1/2}(R)$ , in the first case is  $-\langle \pi_y | h_z^{SO} | \pi_x \rangle$  whereas in the second case it is  $+\langle \pi_y | h_z^{SO} | \pi_x \rangle$ .

This discussion is consistent with the observation by Breckenridge<sup>4</sup> that, based on high-resolution gas phase spectroscopy, for the  $2^1\Pi$  state of the van der Waals molecules  $Na(3p_\pi)Rg$ , for  $Rg = Kr, Xe,^{42,43} Ar,^{44}$  and  $Li(2p_\pi)Rg$ , for  $Rg = Ar,^{45} Ne,^{46}$  the fine-structure splitting is found to be uniformly regular and decreases, from values too large to result from  $M(np_\pi)$  interactions, with increasing  $\nu$ . The  $\nu$  dependence is in accord with our discussion of the  $R$  dependence of the heavy atom effect on the open shell  $\pi$  orbital, in our case the  $3\pi$  orbital. The regular fine-structure splitting is expected, regardless of the atom contributing to heavy atom effect, since the open  $\pi$  shell is less than half full; see the right hand side of eq 8c. In this latter regard, a previous determination of the fine-structure splitting in  $Na(3p_\pi)Ar$  using single-configuration SCF wave functions is illuminating.<sup>47</sup>

ii. *Molecular Orbital Interpretation of the Bonding.* Since the  $8\sigma$  orbital acquires Ar  $3p_z$  character, the corresponding

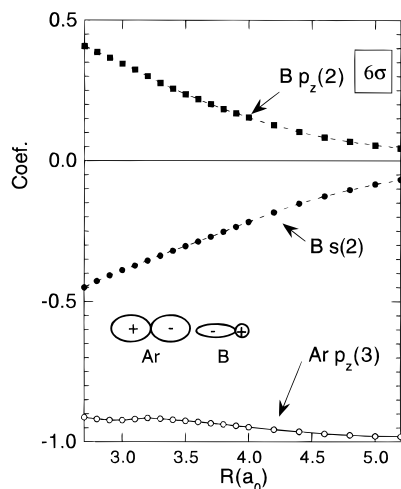


**Figure 8.** Dominant atomic orbital contributions to the  $6\sigma$  (nominally Ar  $3p_z$ ) molecular orbital of BAr from the SA-MCSCF procedure, as a function of internuclear separation. A picture of the orbital arrangement is included.

doubly occupied argon-like orbital, the  $6\sigma$  orbital, should acquire the complementary B  $2p_z$  character. This is in fact the case. Figure 8 shows the three leading atomic orbital contributions to the  $6\sigma$  orbital which is essentially doubly occupied. The Ar  $3p_z$  orbital forms a strong positive overlap with the B  $2p_z$  and B  $2s$  atomic orbitals, a B  $2s2p_z$  hybrid. This can be viewed as Ar furnishing the electrons to the empty B  $2s2p_z$  hybrid orbital to form a coordinate covalent, or dative, bond. B  $2s-2p_z$  hybridization facilitates the dative bonding by both orienting one B  $2s-2p_z$  lobe toward the argon and by permitting the half occupied  $7\sigma$  orbital (nominally the other B  $2s-2p_z$  lobe) to point away from the region of the dative bond.

While the above analysis is suggestive, the importance of the  $6\sigma$  orbital to the bonding was demonstrated by explicit calculations. As noted in section II, if the  $6\sigma$  orbital is not correlated, the  $C^2\Delta$  state is predicted to be essentially unbound. For example, at the FOCI/AVDZ level  $D_e = 3435 \text{ cm}^{-1}$  when the  $6\sigma$  orbital is correlated, that is, included in the active space at the CI level, but only  $26 \text{ cm}^{-1}$  when the  $6\sigma$  orbital is not correlated, that is, removed from the active space at the CI level. Note that in each case the  $6\sigma$  orbital is optimized in the SA-MCSCF procedure. A similar result is found at the SOCI/AVDZ level where the  $D_e = 1459 \text{ cm}^{-1}$  when the  $6\sigma$  orbital is correlated and only  $58 \text{ cm}^{-1}$  when it is not. Finally, even at the MCSCF/TZ1F level where dynamic correlation is modest,  $D_e \approx 500 \text{ cm}^{-1}$  when the MCSCF active space is expanded to include the  $6\sigma$  orbital, but the  $C^2\Delta$  state is unbound when the  $6\sigma$  orbital is excluded from the active space. Recall that, as noted in section II, including the  $6\sigma$  orbital in the MCSCF active space has little effect on a subsequent CI treatment.

This analysis demonstrates the importance of the  $6\sigma$  orbital and electron correlation in the bonding of the  $C^2\Delta$  state. It also shows that unlike a "true" coordinate covalent bond, the bond strength in BAr( $C^2\Delta$ ) is strongly dependent on the level of electron correlation. In this regard Bauschlicher et al.<sup>48</sup> have observed that dative interactions are poorly described at the SCF level. Electron correlation can improve the description of the polarizability of the Ar  $3p$  shell, increasing the opportunity for overlap with the boron. Thus as in BAr  $B^2\Sigma^+$ ,<sup>21</sup>  $D_e(C^2\Delta)$  results from a delicate balance of factors, here predominantly coordinate covalency and electron correlation.

In summary, as  $R$  decreases the fully occupied  $6\sigma$  (Ar  $3p_z$ ) and  $2\pi$  (Ar  $3p_\pi$ ) orbitals mix in B  $2s2p_z$  and B  $2p_\pi$  character in a bonding manner. The corresponding boron-centered orbitals,

the  $8\sigma$  and  $3\pi$ , mix in Ar character in an antibonding manner. In the  $C^2\Delta$  state, the somewhat antibonding  $3\pi$  orbitals are half occupied while the  $8\sigma$  orbital is empty. In addition  $\sigma-\sigma$  overlap is expected to be greater than  $\pi-\pi$  overlap. Thus the predominant contribution to the bonding is expected to come from the  $6\sigma$  orbital, the dative bond. This suggestion, motivated by the analysis of  $H^{SO}(1^4\Pi, C^2\Delta)$ , was confirmed by performing the CI calculations with (binding predicted) and without (binding not predicted)  $6\sigma$  correlation. If this interpretation of the origin of the bonding is correct, other states of BAr with a similar electronic description should also be bound. Referring to the qualitative description of the electronic structure presented in Figure 1, it can be seen that the  $1^4\Sigma^-$  state differs from the  $C^2\Delta$  state only in spin pairing, as both states nominally arise from the  $1s^22s^12p_\pi^2$  configuration of atomic boron. In the single-CSF picture:

$$\Psi_{C^2\Delta_{xy}} \approx \dots 7\sigma \alpha 3\pi_x 3\pi_y (\alpha\beta - \beta\alpha)$$

$$\Psi_{1^4\Sigma^-} \approx \dots 7\sigma \alpha 3\pi_x 3\pi_y (\alpha\beta + \beta\alpha)$$

On the basis of this similarity and our theoretical model of the bonding in the  $C^2\Delta$  state, one would predict that the  $1^4\Sigma^-$  state is bound as well. To test this hypothesis, calculations were performed for BAr( $1^4\Sigma^-$ ) at the FOCI/TZ1F level of theory. At this level of approximation, the  $1^4\Sigma^-$  state is in fact predicted to be bound ( $D_e \approx 2531 \text{ cm}^{-1}$ ,  $R_e \approx 3.95 a_0$ ), supporting our model of the bonding.

As noted above, Massick and Breckenridge<sup>37,38</sup> have reported the existence of a strongly bound doubly excited  $3^3\Sigma^-$  valence state of the neutral van der Waals molecule  $\text{Mg}(3p_\pi^2)\text{Ar}$ ,  $D_e = 2910 \text{ cm}^{-1}$ . This state has a principal electronic configuration analogous to that of  $\Psi_{1^4\Sigma^-}$  without the  $7\sigma$  orbital.<sup>37</sup> Thus the mechanism for bonding suggested here may be operative in  $\text{Mg}(3p_\pi^2)\text{Ar}$  also. On the other hand, there are open shell van der Waals complexes in which this mechanism of the bonding is less likely. Since He has no occupied p orbitals, the  $2^2\Pi$  state of  $\text{Li}(2p)\text{He}$ , which is quite anomalous,<sup>49</sup> falls into this category. Its bonding has been analyzed in terms of a core penetration model.<sup>49</sup>

#### IV. Conclusions

Calculations are reported for atomic boron with six different basis sets and three levels of configuration interaction. In the theoretical description of the nominal valence boron  $1s^22s^12p^2$   $^2D$  state, it was necessary to include near degeneracy effects attributable to the Rydberg  $1s^22s^23d^1$   $^2D$  electron configuration.

Unusually strong binding in the BAr  $C^2\Delta$  electronic state was found. See also refs 3,8. The valence-Rydberg mixing in the B  $^2D$  state is not reflected in the equilibrium structure of BAr( $C^2\Delta$ ). The binding is best described as a dative, or coordinate covalent, bond with the Ar furnishing the electrons from its full occupied  $3p_z$  orbital to an empty B  $2s2p_z$  hybrid orbital. This explanation for the bonding was suggested by the  $1^4\Pi \sim C^2\Delta$  spin-orbit coupling which evinces a significant external heavy atom effect. Overall the binding results from a balance of this bonding interaction and electron correlation effects. It was found that high-order configuration-interaction effects are very important in describing the overall binding and hence  $D_e(C^2\Delta)$ . Similar results have been reported by Hwang et al. for the BAr  $B^2\Sigma^+$  state.<sup>21</sup>

This new bonding model predicts significant binding for BAr( $1^4\Sigma^-$ ). This prediction was confirmed by preliminary calculations. It will be interesting to see whether the bonding model proposed in this work is operative in other open shell

van der Waals complexes. In this regard calculations for the isovalent  ${}^2\Delta$ ,  ${}^4\Sigma^-$  and  ${}^4\Pi$  states in BNe and BKr are being carried out, and calculations on AlNe and AlAr are planned. The  ${}^2\Pi$  state of Li(2p)Ne will also be considered.

**Acknowledgment.** The calculations here were performed on IBM RS/6000 workstations purchased with funds from AFOSR grant AFOSR 90-0051, NSF grant CHE 91-03299, and DOE-BES grant DE-FG02-91ER14189. The authors thank Prof. Millard Alexander for providing electronic copies of the AVDZ and AVTZ basis sets and Prof. Paul Dagdigian and Xin Yang for numerous illuminating discussions and for making their experimental results available prior to publication. K.S. thanks Lisa Pederson for technical assistance.

## References and Notes

- (1) Fajardo, M. E.; Tam, S.; Thompson, T. L.; Cordonnier, M. E. *Chem. Phys.* **1994**, *189*, 351–355.
- (2) Chen, Y.; Hoffmann, G.; Shin, S. K.; Oh, D.; Sharpe, S.; Zeng, Y. P.; Beaudet, R. A.; Wittig, C. In *Advances in Molecular Vibrations and Collision Dynamics*; JAI: Greenwich, 1992; Vol. 1, p 187.
- (3) Dagdigian, P.; Yang, X.; Hwang, E. Non-bonding interactions of the boron atom in the excited  $2s^23s\ ^2S$  Rydberg and  $2s2p^2\ ^2D$  valence states. In *Highly Excited States: Relaxation, Reactions and Structure*; Mullin, A. S., Schatz, G. C., Eds.; ACS Symposium Series; American Chemical Society: Washington, DC, in press.
- (4) Breckenridge, W. H.; Jouvét, C.; Soep, B. *Adv. Met. Semicond. Clusters* **1995**, *3*, 1–83.
- (5) Yang, X.; Hwang, E.; Dagdigian, P. J.; Yang, M.; Alexander, M. H. *J. Chem. Phys.* **1995**, *103*, 2779.
- (6) Yang, X.; Hwang, E.; Dagdigian, P. J. *J. Chem. Phys.* **1996**, *104*, 599.
- (7) Yang, X.; Hwang, E.; Dagdigian, P. J. *J. Chem. Phys.* **1996**, *104*, 8165–8168.
- (8) Yang, X.; Dagdigian, P. J. *J. Chem. Phys.*, in press.
- (9) Sohlberg, K.; Yarkony, D. R. *J. Chem. Phys.*, in press.
- (10) Bruna, P. J.; Peyrimhoff, S. D. *Adv. Chem. Phys.* **1987**, *67*, 1.
- (11) Bauschlicher, C. W.; Langhoff, S. R. *Chem. Rev.* **1991**, *91*, 701.
- (12) Foresman, J. B.; Head-Gordon, M.; Pople, J. A.; Frisch, M. J. *J. Phys. Chem.* **1992**, *96*, 135.
- (13) Fülischer, M. P.; Roos, B. O. *Theor. Chim. Acta* **1994**, *87*, 403–413.
- (14) Kendall, R. A.; Dunning, T. H., Jr.; Harrison, R. J. *J. Chem. Phys.* **1992**, *96*, 6796.
- (15) Odintzova, G. A.; Striganov, A. R. *J. Phys. Chem. Ref. Data* **1979**, *8*, 63.
- (16) Shavitt, I. The Method of Configuration Interaction. In *Modern Theoretical Chemistry*; Schaefer, H. F., Ed.; Plenum Press: New York, 1976; Vol. 3, p 189.
- (17) Docken, K.; Hinze, J. *J. Chem. Phys.* **1972**, *57*, 4928.
- (18) Hinze, J. *J. Chem. Phys.* **1973**, *59*, 6424.
- (19) Diffenderfer, R. N.; Yarkony, D. R. *J. Phys. Chem.* **1982**, *86*, 5098.
- (20) Alexander, M. H. Private communication.
- (21) Hwang, E.; Huang, Y. L.; Dagdigian, P. J.; Alexander, M. H. *J. Chem. Phys.* **1993**, *98*, 8484.
- (22) Dunning, T. H., Jr. *J. Chem. Phys.* **1989**, *90*, 1007.
- (23) Bardo, R. D.; Ruedenberg, K. *J. Chem. Phys.* **1973**, *59*, 5956.
- (24) Silverstone, H. J.; Sinanoglu, O. *J. Chem. Phys.* **1966**, *44*, 1899–1907.
- (25) Langhoff, S. R.; Davidson, E. R. *Int. J. Quantum. Chem.* **1974**, *8*, 61–72.
- (26) Prime, S.; Rees, C.; Robb, M. A. *Mol. Phys.* **1981**, *44*, 173–185.
- (27) Blomberg, M. R. A.; Siegbahn, P. E. M. *J. Chem. Phys.* **1983**, *78*, 5682.
- (28) Wright, J. S.; Kolbuszewski, M. *J. Chem. Phys.* **1993**, *98*, 9725.
- (29) Gleichmann, M. M.; Hess, B. A. *J. Chem. Phys.* **1994**, *101*, 9691.
- (30) Moore, C. E. *Atomic Energy Levels, National Standard Reference Data Series, National Bureau of Standards*; U. S. GPO: Washington, DC, 1971.
- (31) Yarkony, D. R. *Int. Rev. Phys. Chem.* **1992**, *11*, 195–242.
- (32) Hwang, E.; Dagdigian, P. J.; Alexander, M. H. *Can. J. Chem.* **1994**, *72*, 821.
- (33) Bartlett, R. J. Coupled Cluster Theory: An Overview of Recent Developments. In *Modern Electronic Structure Theory*; Yarkony, D. R., Ed.; World Scientific Publishing: Singapore, 1995; Vol. 2.
- (34) Boys, S. F.; Bernardi, F. *Mol. Phys.* **1970**, *19*, 553.
- (35) Malrieu, J. P.; Daudey, J. P.; Caballol, R. *J. Chem. Phys.* **1994**, *101*, 8908.
- (36) Meller, J.; Malrieu, J. P.; Heully, J. L. *Chem. Phys. Lett.* **1995**, *244*, 440–447.
- (37) Massick, S.; Breckenridge, W. H. *J. Chem. Phys.* **1996**, *104*, 7784.
- (38) Massick, S.; Breckenridge, W. H. *J. Chem. Phys.* **1996**, *105*, 6154.
- (39) Heidecke, S. A.; Fu, Z.; Colt, J. R.; Morse, M. D. *J. Chem. Phys.* **1992**, *97*, 1692.
- (40) Duval, M.-C.; D'Azy, O. B.; Breckenridge, W. H.; Jouvét, C.; Soep, B. *J. Chem. Phys.* **1986**, *85*, 6324.
- (41) Esposti, A. D.; Werner, H.-J. *J. Chem. Phys.* **1990**, *93*, 3351.
- (42) Bröhl, B.; Kapetanakis, J.; Zimmerman, D. *J. Chem. Phys.* **1991**, *94*, 5865.
- (43) Braumann, P.; Bröhl, B.; Zimmerman, D. *J. Mol. Spectrosc.* **1992**, *155*, 277.
- (44) Smalley, R. E.; Auerbach, D. A.; Fitch, P. S.; Levy, D. H.; Wharton, L. *J. Chem. Phys.* **1977**, *66*, 3778.
- (45) Bröhl, B.; Zimmerman, D. *Chem. Phys. Lett.* **1995**, *233*, 455.
- (46) Lee, C. J.; Havey, M. D. *Phys. Rev. A* **1991**, *43*, 6066.
- (47) Cooper, D. L. *J. Chem. Phys.* **1981**, *75*, 4157–4159.
- (48) Bauschlicher, C. W., Jr.; Langhoff, S. R.; Partridge, H. The application of ab initio electronic structure calculations to molecules containing transition metal atoms. In *Modern Electronic Structure Theory*; Yarkony, D. R., Ed.; World Scientific Publishing: Singapore, 1995; Vol. 2, pp 1280–1374.
- (49) Bililign, S.; Gutowski, M.; Simons, J.; Breckenridge, W. H. *J. Chem. Phys.* **1994**, *100*, 8212–8218.